Continuous Emulsion Styrene−Butadiene Rubber (SBR) Process: Computer Simulation Study for Increasing Production and for Reducing Transients between Steady States

Roque J. Minari, Luis M. Gugliotta, Jorge R. Vega, and Gregorio R. Meira*

INTEC (Universidad Nacional del Litoral and CONICET), Güemes 3450, (3000) Santa Fe, Argentina

The industrial production of two styrene−butadiene rubber (SBR) grades is optimized by means of a representative mathematical model. The emulsion process involves a train of seven continuously stirred-tank reactors. In the simulations, intermediate feeds of comonomers and chain transfer agent (CTA) are admitted. The steady-state (SS) productions can be increased by ∼8%, while maintaining the required final values of conversion, particle diameter, and molecular characteristics ($\bar{M}_n$, $\bar{M}_w$, and the average number of branches per molecule). For the same rubber grade, the polymer production can be changed with negligible generation of intermediate off-specs, by regulating the global calorimetric conversion. For changes of grade at a fixed polymer production, transient profiles of the intermediate CTA feeds are proposed. For changes of production and grade, a sequential (rather than a simultaneous) transition seems preferable.

Introduction

Styrene−butadiene rubber (SBR) is a general-purpose commodity that is mainly used in the tire industry. It is produced by copolymerizing styrene (S) and butadiene (B) in emulsion processes that are performed in up to 15 continuously stirred tank reactors (CSTRs) in series. Compared to the batch or semibatch processes, continuous processes offer improved efficiency and better product consistency.[1−3] The reagents are continuously fed into the first reactor, and the product (a synthetic latex) is removed from the last reactor. The unreacted monomer then is recuperated from the latex, and the rubber is precipitated and dried.

"Hot" SBR grades are produced at ∼50 °C with persulfate initiators, whereas "cold" grades are synthesized at 5−10 °C, using redox couples. The rubber quality is determined by the molecular weights, chemical composition, and degree of branching. Cold grades are preferable to hot grades, for their reduced levels of branching, cross-linking, and low-molecular-weight material.[2] In industry, the rubber quality is measured by the Mooney viscosity (ASTM D 1646), which is indirectly related to the molecular characteristics and the possible incorporation of (low-molecular-weight) additives.[4,5]

In the investigated cold copolymerizations, the reactivity ratios are relatively similar to unity ($r_B = 1.7$ and $r_S = 0.44$), and this determines a moderate compositional drift, that slightly increases the mass fraction of S in the copolymer. The most common cold SBR grades are known as 1712 and 1502, with the former exhibiting higher molecular weights. Also, grade 1712 includes a mineral oil, whereas no oil is added onto grade 1502. For both grades, the mass fraction of S is ∼23.5%. Molecular branching is due to reactions between the growing free radicals and B repeating units. The molecular weights and branching are controlled by the addition of a chain transfer agent (CTA) or "modifier", and by limiting conversion to ∼70%. The limitation of conversion also limits the gel formation and the compositional drift.[2]

The mathematical modeling of emulsion copolymerizations has been reviewed by Saldívar et al.[6] Emulsion models have been classified according to the way in which they treat the free-radical compartmentalization.[7] The simplest (pseudo-bulk) models estimate the molecular weight distribution (MWD) as in a bulk process,[8] calculating the total number of free radicals from the product between the total number of particles (N_p) and the average number of radicals per particle ($\bar{n}$). If most of the dead polymer is generated by chain transfer to the modifier, then pseudo-bulk models have proven adequate for predicting the produced MWDs.[7,9−17]

The steady-state (SS) control of continuous emulsion processes has been investigated by Poehlein and Dougherty,[3] who intended to increase the polymer production of a single CSTR, by finding the optimal mean residence time (θ) that maximizes N_p. At low θ values, N_p is mainly determined by the initiation rate (R_I), and it is essentially unaffected by the emulsifier concentration. At high θ values, the polymer particles grow to larger sizes, which reduces the total number of soap micelles, and the N_p results are strongly affected by the emulsifier concentration, but unaffected by R_I. The $N_p-\theta$ relationship presents a maximum for systems exhibiting Case II kinetics.[18,19]

Since practically no polymerization occurs in the monomer droplets phase, it is possible to increase the polymer production by reducing the (almost inert) monomer phase in the first reactors of the train. The total monomer phase in the first reactors can be reduced by splitting the feed of comonomer mixture into two or more reactors.[20−23] Thus, Hamielec and MacGregor[20] proposed to split the (unemulsified) monomer feed between the first and fourth reactor in an emulsion copolymerization of S and B that was conducted in a six-reactor train. For splitting ratios 90/10 and 80/20, the polymer production was increased by 3% and 6%, respectively. Also, the branching frequency was practically unaffected, but the average molecular weights were slightly augmented.[20] In addition to splitting the comonomers feed, Penlidis et al.[21] suggested to simultaneously control molecular weights and branching by also splitting the total CTA feed. Furthermore, the copolymer composition could be made more uniform, via intermediate addition of the most reactive comonomer (B).[21] Kanetakis et al.[22] also investigated the increase of productivity by splitting the comonomers feed, showing that the degrees of branching could be reduced when increasing the total inlet flow rate at a fixed monomer conversion.

In industrial practice, the changes of grade and/or of the level of production are rather frequent, for which reason a large

* To whom correspondence should be addressed. Tel.: 0054-342-456-5882. Fax: 0054-342-455-0944. E-mail: gmeira@ceride.gov.ar.

10.1021/ie0504755 CCC: $33.50
Published on Web 11/25/2005

Table 1. Normal SSs Recipes and Final Properties of the Two Investigated Styrene−Butadiene Rubber (SBR) Grades[a]

parameter	SBR grade 1712	SBR grade 1502
q_T [L/min]	423.9	302.8
B [pphm][b]	70.5	71.2
S [pphm]	29.5	28.8
water [pphm]	180.0	200.0
emulsifier[c] [pphm]	4.41	5.36
redox initiator[d] [pphm]	0.067	0.040
CTA[e] [pphm]	0.089	0.182
G [kg/min]	73.9	57.9
x_{sol} [%]	21.2 (**21.3**)	22.6 (**22.8**)
x [%]	56.4 (**56.8**)	65.7 (**64.6**)
N_p/V_w [1/L]	2.396×10^{18}	1.940×10^{18}
$\bar{d}_p$ [nm]	64.5 (**66.3**)	70.3 (**72.5**)
$\bar{p}_S$ [%]	23.1 (**22.9**)	23.1 (**23.1**)
$\bar{M}_n$ [g/mol]	215900 (**211000**)	105000 (**105000**)
$\bar{M}_w$ [g/mol]	996000 (**937000**)	307200 (**282000**)
$(\bar{M}_w/\bar{M}_n)$	4.61 (**4.44**)	2.93 (**2.69**)
$\bar{B}_{n3}$ [molecule^{-1}]	0.249	0.149
$\bar{B}_{n4}$ [molecule^{-1}]	0.094	0.056

[a] Data taken from Gugliotta et al.[17] The predicted values are in normal font, whereas the measured values are presented in parentheses and bold font.[17] [b] Parts per hundred monomer. [c] Sodium soap mixture. [d] *p*-Menthane hydroperoxide. [e] *tert*-Dodecyl mercaptan.

amount of off-spec product is generated during the transients. For reducing the intermediate off-specs, "bang-bang" profiles of the initiator and/or of the CTA feeds into the first reactor are applied.

Calorimetric measurements have been proposed for monitoring and controlling (batch and semibatch) emulsion polymerizations. For example, calorimetric measurements have been used in an industrial copolymerization of acrylonitrile and B, to control conversion and monitor copolymer composition and molecular weights.[24] As far as the authors are aware, this is the first article where calorimetric measurements are proposed for controlling the transients between SSs in a continuous emulsion polymerization.

The present theoretical work is an extension of our previous publications on the same continuous process.[23,25] Our intentions here are (i) to increase the SS production without deteriorating the rubber quality and (ii) to reduce the off-specs that are generated during changes of production and/or of grade. Consider first the investigated plant together with some of our previous developments.

Industrial Process and Our Previous Investigations

Simulated Plant. We have investigated a continuous plant for the production of SBR (grades 1712 and 1502), involving a train of seven identical CSTRs (each of which are the property of Petrobras Energía S. A., Pto. Gral. San Martín, Santa Fe, Argentina). Each reactor exhibits a reaction volume of 17 473 L and operates at a temperature of 10 °C. Their cooling system is described elsewhere.[24,26] It uses a propane−propylene refrigerant that circulates through a set of internal vertical tubes that are arranged to operate as reactor baffles. The reaction heat is removed by evaporation of the refrigerant mixture. The industrial plant does not include intermediate feeds along the train, and the rubber quality is determined from off-line measurements of conversion, copolymer composition, and Mooney viscosity. For any given grade, the final conversion is fixed, irrespective of the level of production. The normal final conversions are limited to 70%, to ensure a negligible production of gel.

Mathematical Model and Normal Plant Operation. Taken from Gugliotta et al.,[17] Table 1 presents the recipes and final properties of grades 1712 and 1502; Figure 1 reproduces some final measurements and simulated profiles of the conversion (x), the polymer production per unit time (G), and the molecular properties. (In Figures 1−4, note that only the points at integer reactor numbers have a physical meaning.) The monomer conversion and the polymer production both grow more or less linearly along the train. In contrast, chain branching exhibits an exponential growth in the last reactors. This is a consequence of two combined effects: a reduced concentration of CTA and an increased concentration of polymer in the polymer particles, after the disappearance of the monomer droplets phase.

The polymerization model is described elsewhere.[17] The model hypotheses are as follows: (a) the polymer particles are generated by micellar nucleation; (b) the comonomers, the initiator (*p*-menthane hydroperoxide), and the CTA (*tert*-dodecyl mercaptane) are distributed between the phases, according to thermodynamic equilibrium, with constant partition coefficients; (c) the moments of the MWD are calculated by assuming a pseudo-bulk homopolymerization, and the molecular weights are determined by chain transfer reactions; (d) trifunctional branches are produced by chain transfer to the polymer, which, in turn, is caused by hydrogen abstraction from B repetitive units; (e) tetrafunctional branches are produced by the reaction

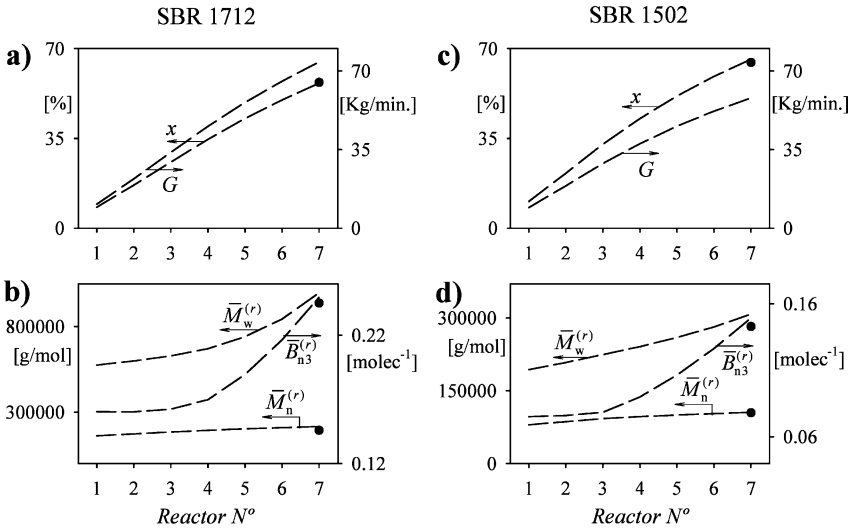

Figure 1. Measurements and model predictions for the normal steady states (SSs) of grades 1712 and 1502 (that do not include intermediate additions of comonomers and a chain transfer agent (CTA)): (a) monomer conversion and polymer production for grade 1712; (b) number- and weight-average molar masses, and average number of trifunctional branches per molecule, for grade 1712; (c) monomer conversion and polymer production, grade 1502; and (d) number- and weight-average molar masses, and average number of trifunctional branches per molecule, for grade 1502. [After Gugliotta et al.[17]]

between growing free radicals and internal double bonds of B units; and (f) there is a negligible generation of gel.

The model was subdivided into two modules in series: a Basic Module, which predicts conversion x, number-average particle diameter $\bar{d}_p$, and the average weight fraction of S in the copolymer ($\bar{p}_S$); and a Molecular Weights Module, which predicts average molecular weights ($\bar{M}_n$ *and* $\bar{M}_w$) and the average number of trifunctional and tetrafunctional branches per molecule ($\bar{B}_{n3}$ and $\bar{B}_{n4}$, respectively).[17] The Basic Module is based on a kinetic scheme that considers (a) in the aqueous phase, redox initiation and deactivation of free radicals by O_2; and (b) in the polymer phase, propagation and termination. The Molecular Weights Module considers the following reactions in the polymer phase: propagation, chain transfer (to the comonomers, to the CTA, and to the polymer), and reactions involving impurities and internal B double bonds.

The model was validated with SS and transient measurements of grades 1502 and 1712. The SS experiments included measurements of conversion, copolymer composition, particle diameter, and average molecular weights along the reactor train.[17] The transient experiment involved final product measurements of the solids content and average molecular weights during a change of grade from 1712 into 1502.[17]

Other model predictions were as follows:[17] (i) all the polymer particles are generated in the first reactor, and for this reason the (unswollen) number-average particle diameter $\bar{d}_p$ increases monotonically along the train; (ii) the investigated process exhibits a Case II kinetics, with $\bar{n} \cong 0.5$; (iii) the mass fraction of S in the copolymer ($\bar{p}_S$), moderately increases along the train; (iv) in the SS of grade 1502, the total volume of monomer phase was 8118 L, distributed among the first two reactors, whereas in the SS of grade 1712, the total volume of monomer phase volume was 12 140 L, distributed among the first three reactors; and (v) the number of tetrafunctional branches per molecule $\bar{B}_{n4}$ is considerably lower than $\bar{B}_{n3}$ (the last two rows of Table 1).

As a consequence of the model prediction that the polymer particles are only generated in the first reactor, then the particle concentration is constant along the train when expressed in the format (N_p/V_w), where V_w is the volume of the aqueous phase. The constant particle concentration was indirectly validated from measurements of the average particle diameter and the conversion along the train. The Case II kinetics with $\bar{n} \cong 0.5$ is a consequence of the following: (a) the small particle diameters observed in the investigated process; (b) the negligible desorption of hydrophobic radicals; (c) the high rate of termination in the polymer phase; and (d) the redox couple is only soluble in the water phase, and, therefore, there is a negligible decomposition of initiator in the polymer particles.[17] The evolutions involving $\bar{B}_{n4}$ are calculated by our model. However, because of the relation $\bar{B}_{n3} > \bar{B}_{n4}$, only the results involving $\bar{B}_{n3}$ will be discussed in all that follows.

To solve the Molecular Weights Module, the outputs from the Basic Module are required, but the Basic Module does not require of the outputs from the Molecular Weights Module. The reasons for this are as follows: (a) the molecular weights are mainly determined by chain transfer to the CTA, and chain transfer reactions do not affect the concentration or reactivity of the free radicals contained in the polymer particles; and (b) CTA radicals do not desorb from the polymer particles. This decoupling of the Basic Module results, with respect to the Molecular Weights Module, makes it possible to adjust conversion and particle size independently from the molecular characteristics.

Vega et al.[25] described the plant policies for changes of production and grade. The plant policy for changes of production is as follows: (a) at $t = 0$, modify the initiator feed to its new value; and (b) after a time equal to one-half the residence time of the reactor train, change all the other feeds into their new values. The plant policy for changes of grade is as follows: (a) modify the initiator feed at $t = 0$; ((b) apply a bang-bang profile to the CTA feed flow, with an intermediate period at a maximum (when the change of grade involves reducing the molecular weights), and at a minimum value (when it involves increasing the molecular weights); and (c) modify all the other feeds after two residence times of any individual CSTR. For the changes of production, no intermediate off-specs are recollected. For the changes of grade, the intermediate off-specs are recollected between the moment when the Mooney viscosity measurement is out of specification of the initial grade, and the moment when the Mooney viscosity measurement is within specification of the final grade. Through this procedure, the off-specs accumulation periods were typically around 8 h of continuous plant operation.

Improved Operations with Intermediate Additions of Comonomers Mixture and CTA. The aims of this paper are as follows: (1) to maximize the SS production without affecting the normal SS values of conversion, the latex properties, and the molecular characteristics; and (2) to minimize the off-spec transient that is produced after changes of grade and/or changes in the level of production. The final conversion is fixed in all cases, because of the large influence of this variable on the product characteristics. Also, the final particle diameter (and the final particle concentration) are imposed fixed at their normal SS values, to avoid affecting the final latex stability.

In regard to aim (1), Vega et al.[23] proposed the following calculation procedure: (i) increase the SS production by reducing the inert monomer droplets phase in the first reactors through splitting the comonomers feed and increasing the total feed flow, while maintaining the normal SS values of the emulsifier feed concentration, conversion, and average particle diameter; (ii) inject intermediate feeds of CTA along the reaction train to produce a constant profile of $\bar{M}_n$; (iii) except for the CTA (where no restrictions were imposed), all the other global input concentrations were maintained at their normal SS values; and (iv) the composition of the comonomer mixture feeds was also fixed at its Normal SS value. The procedure yielded an increased production, but at the cost of deteriorating some of the molecular properties.

In the SS, all the polymer particles are generated in the first reactor, and the ratio N_p/V_w is constant along the train.[17] This suggests the following calculation method for step (i) above:[23] (a) in the first reactor, produce the required N_p/V_w by appropriately increasing the total feed rate while simultaneously reducing the feed of comonomers mixture; (b) in reactors 2, 3, etc., feed the remaining flow rate of comonomers mixture, to produce an almost negligible volume of monomer droplets phase V_m (however, a minor amount of monomer droplets phase is necessary, to ensure saturation of the polymer particles by the comonomers, thus maximizing the polymerization rate); and (c) check the final monomer conversion and iterate until convergence.

In regard to aim (2), Vega et al.[25] theoretically investigated the reduction of off-specs generated between SSs. For changes in production at a given grade, the off-specs could be almost eliminated by first changing the initiator feed at $t = 0$ and then manipulating the total feed flow into the first reactor with a virtual closed-loop controller, with the intention of regulating

Table 2. Operating Conditions and Final Properties for the Investigated Steady States

(a) Grade 1712

	normal SS [a]	SS1a (7 reactors) $\bar{M}_n^{(r)}$ [b]	SS2a (7 reactors) $\bar{M}_w^{(r)}$ [b]	SS3a (7 reactors) $\bar{B}_{n3}^{(r)}$ [b]	SS4a (8 reactors) $\bar{B}_{n3}^{(r)}$ [b]	SS2b (7 reactors) $\bar{M}_w^{(r)}$ [b]
q_T [L/min]	423.9	465.5	465.5	465.5	465.5	321.7
initiator [pphm][c]	0.067	0.067	0.067	0.067	0.067	0.028
$G^{(7)}$ [kg/min]	73.916	81.283	81.283	81.283	88.900	56.160
$\sum_r F_X^{(r)}/G^{(7)}$	1.55×10^{-3}	1.54×10^{-3}	1.62×10^{-3}	1.69×10^{-3}	1.55×10^{-3} [d]	1.58×10^{-3}
$x^{(7)}$ [%]	**56.4**[b]	**56.5**	**56.5**	**56.5**	61.8[d]	**56.5**
$(N_p/V_w)^{(7)}$ [$\times 10^{-18}$ L^{-1}]	**2.396**[b]	**2.398**	**2.398**	**2.398**	2.398[d]	**1.670**
$\bar{d}_p^{(7)}$ [nm]	**64.5**[b]	**64.5**	**64.5**	**64.5**	66.5[d]	**72.8**
$\bar{M}_n^{(7)}$ [g/mol]	**215900**	**215700**	203900	194000	199800[d]	210800
$\bar{M}_w^{(7)}$ [g/mol]	**996000**	1505100	**951400**	813900	953200[d]	947600
$(\bar{M}_w^{(7)})/(\bar{M}_n^{(7)})$	4.61	6.98	4.67	4.19	4.77[d]	4.49
$\bar{B}_{n3}^{(7)}$ [molecule^{-1}]	**0.249**	0.260	0.246	**0.234**	0.265[d]	0.244
$\bar{p}_S^{(7)}$ [%]	23.1	23.2	23.2	23.2	23.5[c]	23.1
$\Delta\bar{p}_S$ [%][e]	0.91	0.68	0.68	0.68	0.99[d]	0.79

(b) Grade 1502

	Normal SS[a]	SS5b (7 reactors) $\bar{M}_n^{(r)}$ [b]	SS6b (7 reactors) $\bar{M}_w^{(r)}$ [b]	SS7b (7 reactors) $\bar{B}_{n3}^{(r)}$ [b]	SS8b (8 reactors) $\bar{B}_{n3}^{(r)}$ [b]	SS6a (7 reactors) $\bar{M}_w^{(r)}$ [b]
q_T [L/min]	302.8	321.7	321.7	321.7	321.7	465.5
initiator [pphm][c]	0.040	0.040	0.040	0.040	0.040	0.097
$G^{(7)}$ [kg/min]	57.900	61.566	61.566	61.566	66.583	89.25
$\sum_r F_X^{(r)}/G^{(7)}$	2.78×10^{-3}	2.78×10^{-3}	2.81×10^{-3}	3.10×10^{-3}	2.87×10^{-3} [d]	2.83×10^{-3}
$x^{(7)}$ [%]	**65.7**[b]	**65.5**	**65.5**	**65.5**	70.9[d]	**65.6**
$(N_p/V_w)^{(7)}$ [$\times 10^{-18}$ L^{-1}]	**1.940**[b]	**1.934**	**1.934**	**1.934**	1.934[d]	2.793
$\bar{d}_p^{(7)}$ [nm]	**70.3**[b]	**70.4**	**70.4**	**70.4**	72.3[d]	62.3
$\bar{M}_n^{(7)}$ [g/mol]	**105000**	**104900**	103100	93400	95500[d]	101800
$\bar{M}_w^{(7)}$ [g/mol]	**307200**	310600	**302900**	264200	286100[d]	303000
$(\bar{M}_w^{(7)})/(\bar{M}_n^{(7)})$	2.93	2.95	2.94	2.83	3.00[d]	2.98
$\bar{B}_{n3}^{(7)}$ [molecule^{-1}]	**0.149**	0.152	0.149	**0.135**	0.156[d]	0.152
$\bar{p}_S^{(7)}$ [%]	23.1	22.9	22.9	22.9	23.3[d]	23.2
$\Delta\bar{p}_S$ [%][e]	1.56	1.30	1.30	1.30	1.71[d]	1.22

[a] It does not include intermediate feeds of comonomer and/or CTA. [b] Restriction imposed when calculating the CTA feeds. [c] All of the other reagents maintain the pphm values of the normal SS (see Table 1). [d] Eighth reactor value. [e] Compositional drift (total variation along the train of the mass fraction of S in the copolymer).

a constant global conversion.[25] For changes of grade at a given production, and by introducing an independent (and transient) feed of CTA into the last reactor, rapid transitions into the final $\bar{M}_n$ values could be achieved. However, the other molecular properties ($\bar{M}_w$ and $\bar{B}_{n3}$) remained out of specification for longer periods, with the result of an almost negligible reduction of the off-specs with respect to the plant policy.

Improved Steady States

Increase of Production while Maintaining Conversion and All the Other Quality Properties as in Their Normal SSs. Consider intermediate additions of comonomers mixture and CTA along the train. The SS optimizations exhibit the following common features: (a) the increase of production is restricted to maintaining the same final values for x, N_p/V_w, and $\bar{d}_p$ of the normal SS operation; and (b) except for the CTA (where no consumption restrictions were imposed), the inlet concentrations of all the other reagents were maintained at the normal SS values of Table 1. The following two-step procedure was applied. First, following Vega et al.,[23] increase the total feed rate q_T and simultaneously split the mass flow of comonomers mixture into the first reactors of the train [we call this $F_M^{(r)}$ with ($r = 1, 2, ...$) the mass flow rate of comonomers mixture into reactors 1, 2,...]. Second, manipulate the CTA feeds $F_X^{(r)}$ ($r = 1, 2, ...$) to reproduce the (normal SS) profiles of either $\bar{M}_n$, $\bar{M}_w$, or $\bar{B}_{n3}$ of Figures 1b and 1d, while observing the final values of the other two molecular characteristics. Instead of requiring predetermined profiles of $\bar{M}_n$, $\bar{M}_w$, or $\bar{B}_{n3}$, we would really want to produce all three of the final molecular characteristics of the normal SSs. However, this is impossible to obtain by only modifying the SS concentrations of CTA along the train. Also, the comonomer feeds $F_M^{(r)}$ must be maintained fixed, to ensure the required final conversion and particle size. In relation to the second step, the numerical algorithms that have been applied to calculate the CTA feeds are presented in Appendix A. More specifically, eq A.13 was used in combination with eqs A.10, A.11, or A.12, to produce controlled profiles of either $\bar{M}_n^{(r)}$, $\bar{M}_w^{(r)}$, or $\bar{B}_{n3}^{(r)}$. The SS results are presented in Figures 2−4 and Table 2 under SS1a, SS2a, SS3a, SS5b, SS6b, and SS7b. The intention of the steady states indicated by SS1a and SS5b is to reproduce the $\bar{M}_n$ profiles of the normal SSs (Figure 2). The intention of the steady states indicated by SS2a and SS6b is to reproduce the $\bar{M}_w$ profiles of the normal SSs (Figure 3). The intention of the steady states indicated by SS3a and SS7b is to reproduce the $\bar{B}_{n3}$ profiles of the normal SSs (Figure 4).

Through application of the first step, it resulted that the comonomer mixture must be injected into the first four reactors, with the largest SS feed applied onto the second reactor (see Figure 2a and d, Figure 3a and d, and Figure 4a and d). As required, the final values of x, N_p/V_w, and $\bar{d}_p$ almost coincide with the normal SS values (also reproduced in the second column of Table 2). The total feed q_T was increased from 423.9 to 465.5 L/min for grade 1712, and from 302.8 to 321.7 L/min for grade 1502. Correspondingly, the polymer productions were increased by 10% and 6.3%, respectively (shown in the upper rows of Table 2a and b). The comonomer feed profiles of

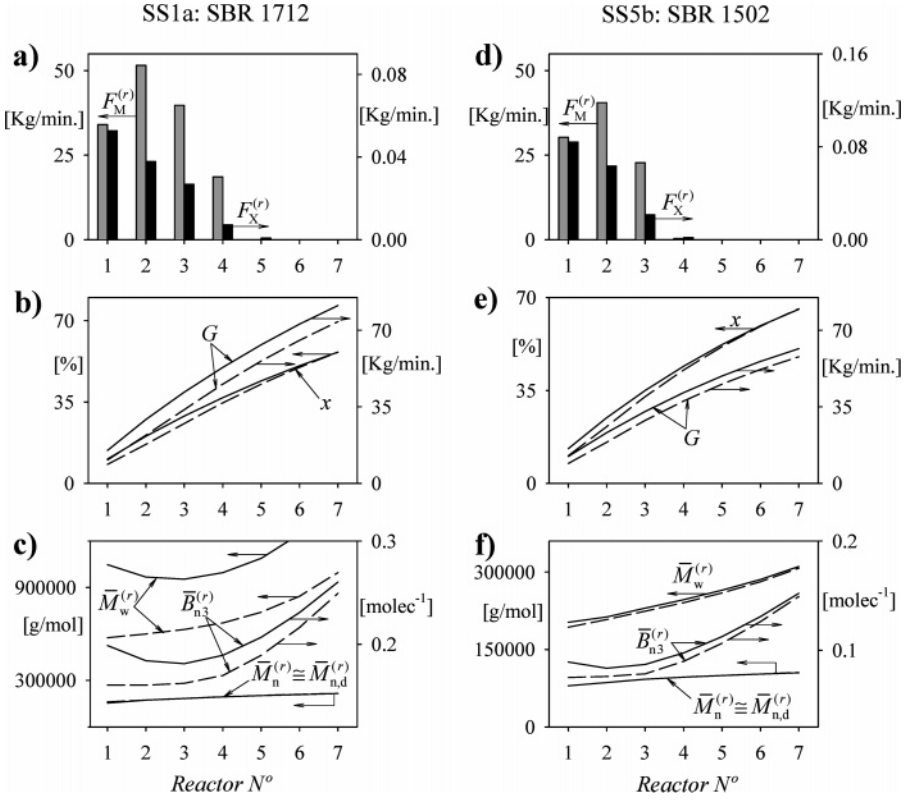

Figure 2. Optimal SSs obtained by imposing the $\bar{M}_n^{(r)}$ profile of the normal SS operation (shown as a continuous trace). For comparison, the normal SS profiles are also presented (shown as a dashed trace). For SS1a, grade 1712: (a) monomer and CTA feed profiles, (b) monomer conversion and polymer production, and (c) number- and weight-average molecular weights and average number of trifunctional branches per molecule. For SS5b, grade 1502: (d) monomer and CTA feed profiles, (e) monomer conversion and polymer production, and (f) number- and weight-average molecular weights and average number of trifunctional branches per molecule.

Figures 2a, 3a, and 4a all coincide; the same also is true for the comonomer profiles of Figures 2d, 3d, and 4d. The reason is that conversion and particle density are fixed for any given grade. In the first reactor, the total feed flow q_T and feed of comonomer mixture $F_M^{(1)}$ were adjusted to provide the desired final value of N_p/V_w. In reactors 2, 3, etc., the comonomer feeds $F_M^{(r)}$ ($r = 2, 3, 4$) were adjusted to minimize (but not eliminate) their monomer phase volumes.

The required CTA feeds were obtained through application of the second step, with the result of decreasing CTA profiles for all the simulated examples (see Figure 2a and d, Figure 3a and d, and Figure 4a and d). Note that a perfect solution was only possible for the SS control of $\bar{M}_n^{(r)}$ (see Figure 2c and f). For the controls of $\bar{M}_w^{(r)}$ or $\bar{B}_{n3}^{(r)}$, the desired values were only achieved in the first reactors but could not be met in the last reactors, where the CTA concentrations were higher than required (see Figures 3c, 3f, 4c, and 4f). As mentioned previously, this problem cannot be solved by feeding additional comonomers mixture into the last reactors, because this would affect the final conversion and the particle diameters. We have defined the CTA efficiency as the ratio between the total CTA mass flow and the polymer production ($\sum_r F_X^{(r)}/G$). For the control of $\bar{M}_n^{(r)}$, $\sum_r F_X^{(r)}/G$ almost coincides with the normal SS value, but it is somewhat higher for the control of $\bar{M}_w^{(r)}$ and $\bar{B}_{n3}^{(r)}$ (see Table 2).

Despite the perfect $\bar{M}_n^{(r)}$ control, the other final molecular qualities are deteriorated as follows: the final values of $\bar{M}_w$ and $\bar{B}_{n3}$ are well above their normal SS values, and the final polydispersity of SS1a is almost 7 (see Figure 2 and Table 2).

The results of imposing $\bar{M}_w^{(r)}$ are presented in Figure 3 and Table 2. The $\bar{M}_w^{(r)}$ values are as required in the first five reactors, but are below the normal SS values in the last two reactors. However, the final polydispersities and $\bar{B}_{n3}$ values are close to their desired values (see Table 2 and Figures 3c and f). Thus, except for the deviations in the molecular weights, the products are within specification, with respect to their polydispersities and levels of branching.

The results of imposing $\bar{B}_{n3}^{(r)}$ are shown in Figure 4 and Table 2. As noted previously, the desired profiles are only met in the first reactors, whereas, in the last reactors, the molecular weights and branching are below their normal SS values. Note however that it is desirable to produce a less-branched final rubber.

In summary, the following can be noted:

(1) In all three cases, the polymer production is increased between 6% and 10%, with respect to the normal SS, while simultaneously reducing the compositional drift $\Delta\bar{p}_S$ (see the last rows of Table 2a and 2b).

(2) The $\bar{M}_n^{(r)}$ control strategy meets with the profile objectives; however, it does produce a deteriorated polymer, from the points of view of the final polydispersity and branching.

(3) The $\bar{M}_w^{(r)}$ strategy is the best for reproducing the required final molecular properties, and for this reason, the SS operations indicated with SS2a and SS6b in Table 2 were adopted as the base conditions for the dynamic optimizations, which are presented below.

(4) The $\bar{B}_{n3}^{(r)}$ strategy reduces the levels of branching, with respect to the normal SS, but at the cost of reducing the molecular weights. Through the $\bar{B}_{n3}^{(r)}$ strategy, the desired final molecular characteristics of the normal SS could be produced by operating at higher conversions. This is discussed in what follows.

Increase of the Final Conversion without Deterioration of the Molecular Properties. The low levels of branching

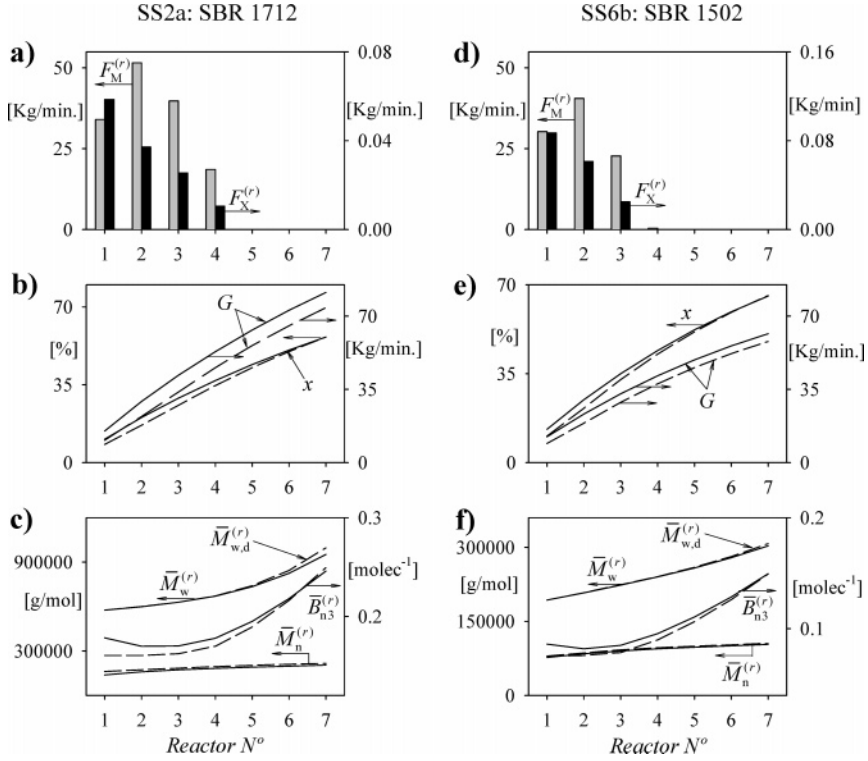

Figure 3. Optimal SSs obtained by imposing the $\bar{M}_w^{(r)}$ profile of the normal SS operation (shown as a continuous trace). For comparison, the normal SS profiles are also presented (shown as a dashed trace). For SS2a, grade 1712: (a) monomer and CTA feed profiles, (b) monomer conversion and polymer production, and (c) number- and weight-average molecular weights and average number of trifunctional branches per molecule. For SS6b, grade 1502: (d) monomer and CTA feed profiles, (e) monomer conversion and polymer production, and (f) number- and weight-average molecular weights and average number of trifunctional branches per molecule.

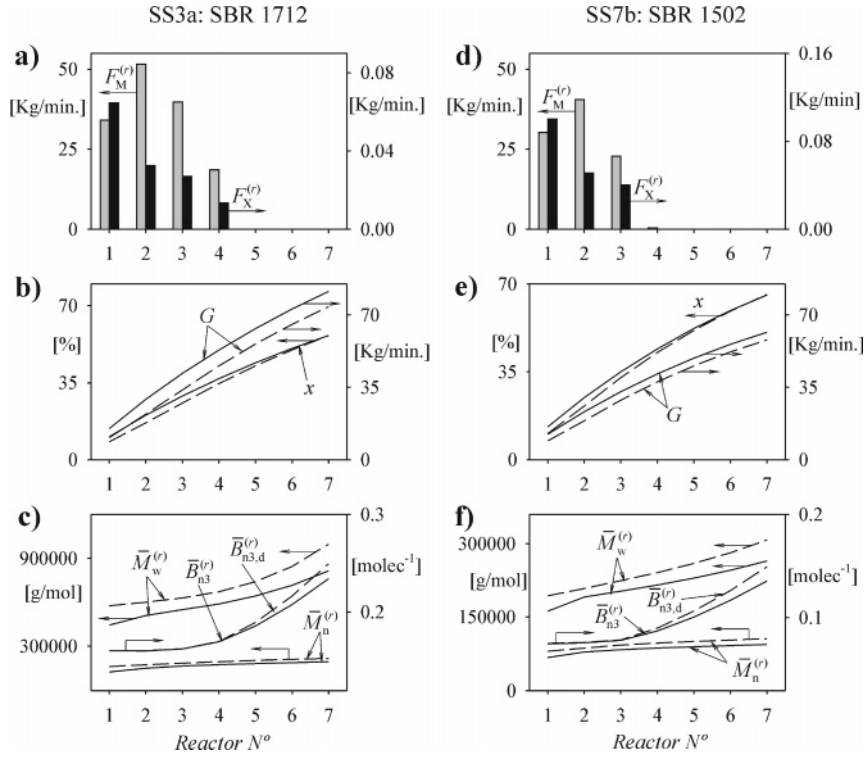

Figure 4. Optimal SSs obtained by imposing the $\bar{B}_{n3}^{(r)}$ profile of the normal SS operation (shown as a continuous trace). For comparison, the normal SS profiles are also presented (shown as a dashed trace). For SS3a, grade 1712: (a) monomer and CTA feed profiles, (b) monomer conversion and polymer production, and (c) number- and weight-average molecular weights and average number of trifunctional branches per molecule. For SS7b, grade 1502: (d) monomer and CTA feed profiles, (e) monomer conversion and polymer production, and (f) number- and weight-average molecular weights and average number of trifunctional branches per molecule.

observed in SS3a and SS7b suggest an increase in the final conversion, with respect to the normal SSs. To this effect, we considered incorporating an extra (eighth) reactor into the train. Even though this modification increases the total reaction volume, it is a practical possibility in industry, where only a fraction of the total available reactors are normally in use. For

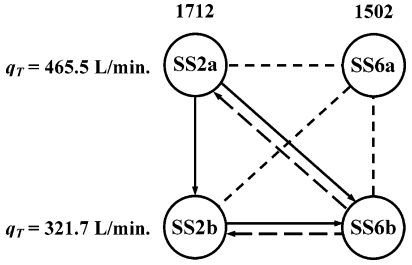

Figure 5. Schematic representation of the investigated transitions between optimal SSs.

an eight-reactor train, the SS simulations with control of the $\bar{B}_{n3}$ profile are presented in Table 2, under SS4a and SS8b. Compared with the normal SSs of the seven-reactor train, the following is observed: (a) the final conversions are increased by more than 5%, and the products exhibit almost perfect specifications with respect to $\bar{M}_n$, $\bar{M}_w$, and $\bar{B}_{n3}$; (b) the productions increase by ~20% for the 1712 grade, and by ~15% for the 1502 grade; and (c) the consumption of CTA per unit polymer mass is practically identical (see Table 2).

Reduction of Transients between Optimal Steady States

Consider reduction of the transients between optimal SSs during changes of (1) production at a fixed grade, (2) grade at a fixed production; and (3) production and grade. The selected base optimal SSs are SS2a, SS6a, SS2b, and SS6b of Table 2, and the investigated transitions are schematized in Figure 5. All four base SSs are optimal in the sense of increasing production while imposing the $\bar{M}_w^{(r)}$ profile of their normal SSs. The SSs indicated by SS2a and SS2b both produce grade 1712, but at different total flow rates and at different productions (since the conversion is fixed); and similarly, grade 1502 is produced from SS6a and SS6b. The new SSs indicated by SS2b and SS6a were obtained based on SS2a and SS6b, by first adjusting q_T, then adjusting the required initiator feed (to produce a constant conversion), and finally applying the previously described $\bar{M}_w^{(r)}$ strategies in an iterative fashion.

To quantify the intermediate off-specs, we considered that the final product is out of specification of the initial grade when any of its molecular properties ($\bar{M}_n$, $\bar{M}_w$, $\bar{M}_w/\bar{M}_n$, or $\bar{B}_{n3}$) fall outside of ±10% of their desired values. Similarly, the outlet product is within specifications of the final grade when all of its molecular properties are within ±10% of their desired values.

Change of Production at a Fixed Rubber Grade. Consider minimizing the off-specs generated during changes of production, at a fixed rubber grade, from SS2a to SS2b. At $t = 0$, only the initiator feed is modified into its final value (Table 2a). The desired values of the initial and final monomer conversion are identical, which suggests that the off-specs can be reduced through a transient closed-loop regulation of the global monomer conversion. We choose the total feed rate (q_T) as the manipulated variable, for its rapid effect on the overall residence time (and, therefore, on conversion). Simultaneously, we propose to modify all the intermediate comonomer and CTA feeds, by applying the same fractional variations of q_T. Instead of the global gravimetric conversion, we propose to regulate the global calorimetric conversion x_c; because this last variable is easily calculated from on-line estimations of the total heating rate Q_R^T [eq B.2]. The total heating rate is estimated by simple addition of the heating rates into each of the reactors; and these, in turn, are obtained from on-line measurements of their evaporated refrigerant flows, the inlet and outlet temperatures, etc. [see the energy balance of eq B.1.a]. However, to simplify

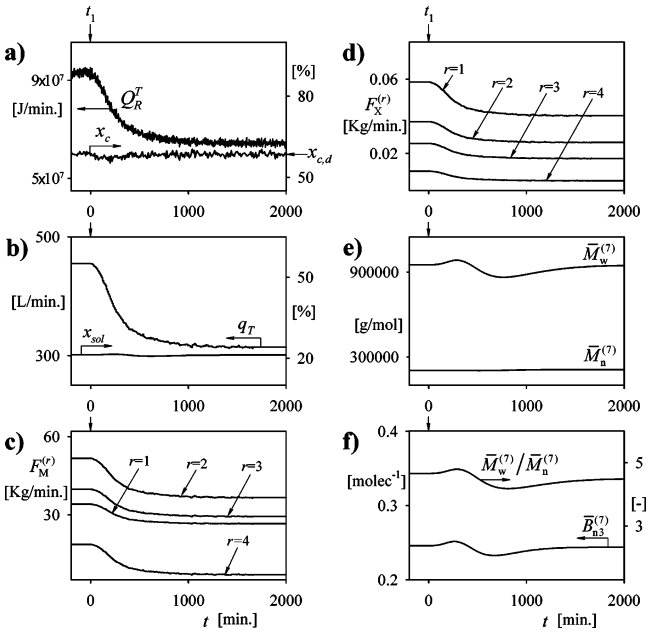

Figure 6. Change of production for grade 1712 with regulation of the calorimetric conversion: (a) simulated Q_R^T "measurement" and regulated x_c; (b) resulting q_T and evolution of $x_{sol}^{(7)}$; (c and d) monomer and CTA feeds profiles into reactors 1, 2, 3, and 4; (e and f) evolutions of the final $\bar{M}_n^{(7)}$, $\bar{M}_w^{(7)}$, $\bar{M}_n^{(7)}/\bar{M}_w^{(7)}$, and $\bar{B}_{n3}^{(7)}$. The initiator step change is applied at $t_1 = 0$ min.

the simulation process, we have estimated the total heating rate directly from eqs B.1b−e. The final Q_R^T estimates include a 2-min "measurement" lag, and an (additive and zero-mean) "measurement" noise.[26] The applied P+I algorithm is represented by eq B.3. The manipulated feeds (q_T, $F_M^{(r)}$, and $F_X^{(r)}$) were readjusted every 10 min., from averaged "measurements" of Q_R^T.

The results of the transition SS2a → SS2b are shown in Figure 6. The desired calorimetric conversion $x_{c,d} = 58.5\%$ corresponds to a gravimetric conversion of $x = 56.4\%$. The controller settings were adjusted to provide a fast response, yielding $K_{P,1} = 3.0$ L/min; and $\tau_{I,1} = 0.15$ min. Figure 6a presents the Q_R^T estimates and the derived calorimetric conversion. The total feed rate q_T and the intermediate feeds of comonomer and CTA are represented in Figures 6b, c, and d, respectively. In the last reactor, the profiles of $x_{sol}^{(7)}$ (Figure 6b), $\bar{M}_n^{(7)}$ and $\bar{M}_w^{(7)}$ (Figure 6e), and $\bar{B}_{n3}^{(7)}$ and $\bar{M}_w^{(7)}/\bar{M}_n^{(7)}$ (Figure 6f) are all smooth, although the feed flows q_T, $F_M^{(r)}$, and $F_X^{(r)}$ are somewhat oscillating. From the evolution of the final molecular variables, the maximum deviation of a quality variable with respect to its (constant) SS value was ~9% for $\bar{M}_w$. Thus, none of the quality variables have fallen outside their ±10% limits, and, therefore (according to our criterion), no off-spec rubber has been produced during the transition.

Finally, an adaptation of the (bang-bang and open-loop) plant policies were simulated. The plant policies were adapted to include the intermediate SS feeds of comonomers and CTA. The initiator recipe was changed at $t = 0$, whereas all the other feeds were changed in a step fashion after one-half residence time of the complete train. The results are presented in Figure 7. The transitions are quite rapid, and comparable to the feedback results of Figure 6. Also, the evolution of Q_R^T in Figure 7a is similar to that of Q_R^T in Figure 6a, even though a step change (rather than a smooth transition) was applied to q_T. From the evolution of the final molecular variables, the maximum observed deviation was 6% for $\bar{M}_w$. Thus, again no off-spec

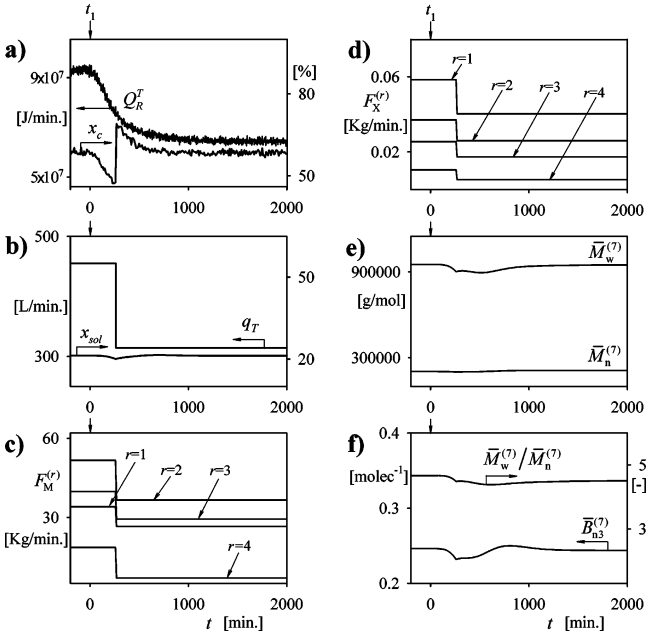

Figure 7. Change of production for grade 1712 with the adopted plant policy: (a) simulated Q_R^T "measurement" and evolution of x_c; (b) resulting q_T and evolution of $x_{sol}^{(7)}$; (c and d) monomer and CTA feeds profiles into reactors 1, 2, 3, and 4; (e and f) evolutions of the final $\bar{M}_n^{(7)}$, $\bar{M}_w^{(7)}$, $\bar{M}_n^{(7)}/\bar{M}_w^{(7)}$, and $\bar{B}_{n3}^{(7)}$. The initiator step change is applied at $t_1 = 0$ min.

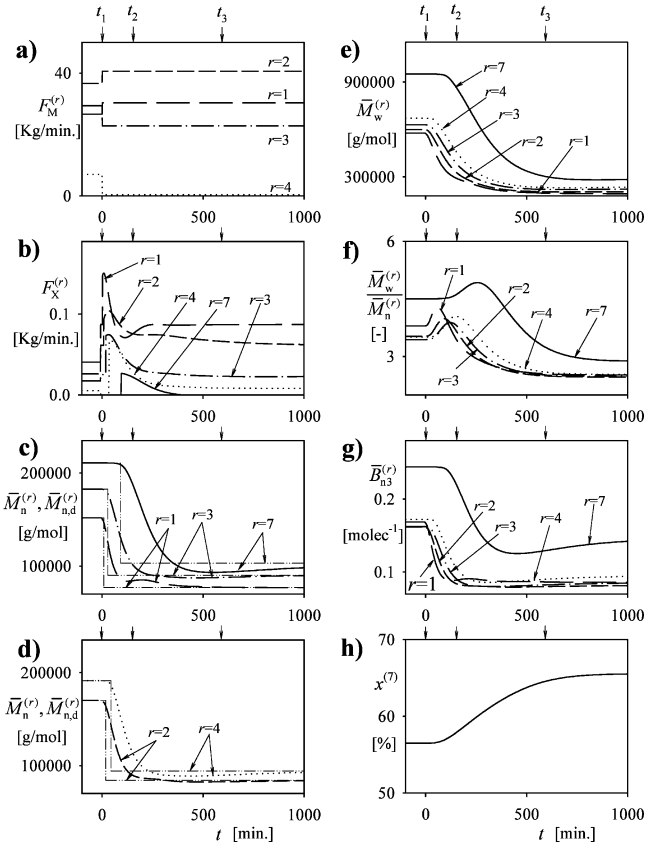

Figure 8. Change of grade from SS2b (grade 1712) into SS6b (grade 1502), with $\bar{M}_n^{(r)}$ control in reactors 1, 2, 3, 4, and 7. The off-spec product is accumulated between $t_2 = 152$ and $t_3 = 594$ min: (a) step change at $t = 0$ of the comonomers feed into reactors 1, 2, 3, and 4; (b) CTA feed profiles into reactors 1, 2, 3, 4, and 7; (c and d) sequential set points changes of $\bar{M}_{n,d}^{(r)}$, and evolution of $\bar{M}_n^{(r)}$ in reactors 1, 2, 3, 4, and 7; (e−g) evolution of $\bar{M}_w$, $\bar{M}_w^{(r)}/\bar{M}_n^{(r)}$, and $\bar{B}_{n3}^{(r)}$ in reactors 1, 2, 3, 4, and 7; and (h) evolution of the final monomer conversion. At $t_1 = 0$ min, a step change in the recipe is introduced.

product has been produced according to the adopted criterion. The adapted bang-bang strategy produces similar results to those of the closed-loop strategy. However, the closed-loop control exhibits the potential advantage of compensating for unknown perturbations in the reagents and/or in the process variables.

Change of Grade at a Fixed Polymer Production. The different grades exhibit variations in the molecular characteristics $\bar{M}_n$, $\bar{M}_w$, and $\bar{B}_{n3}$. We propose to reduce the transitions during changes of grade (at a fixed polymer production), by sequential manipulation of the CTA feeds into reactors 1, 2, 3, 4, and 7. Reactors 1−4 were selected because they already receive CTA feeds in their SS operations. The additional (and transient) feed of CTA into the last reactor is aimed at accelerating the change into the final SS. The CTA feeds can be added but not extracted; and for this reason, the changes of grade that involve a reduction of the average molecular weights are simpler to perform a priori, with respect to those that involve an increase.

To calculate the required CTA feeds, five virtual controllers were implemented. The controlled variables were either $\bar{M}_n^{(r)}$ or $\bar{M}_w^{(r)}$ ($r = 1, 2, 3, 4, 7$). The additions of CTA affect $\bar{M}_n$ more than $\bar{M}_w$, whereas the contrary occurs for CTA reductions. Thus, the control of $\bar{M}_n^{(r)}$ ($r = 1, 2, 3, 4, 7$) was proposed for the transitions involving a molecular weights reduction while the control of $\bar{M}_w^{(r)}$ ($r = 1, 2, 3, 4, 7$) was proposed for the transitions involving a molecular weights increase. Finally, note that the proposed strategy is only developed as a mathematical tool for calculating the required transient feed profiles, with the idea of eventually applying such profiles in an open-loop manner.

Consider the transitions SS2b → SS6b, and vice versa (Figures 8 and 9). The simulation procedure was as follows: (a) at $t = 0$, the initial recipe was modified into the final recipe in a step change; (b) the controlled variables were $\bar{M}_n^{(r)}$ for the transition SS2b → SS6b, and $\bar{M}_w^{(r)}$ for the transition SS6b → SS2b; (c) along the transients, independent P+I controllers were sequentially connected onto reactors 1, 2, 3, 4, and 7, when the relative error between the ($\bar{M}_n^{(r)}$ or $\bar{M}_w^{(r)}$) measurement and its initial SS value was greater than ±5% [see eqs B.4 and B.5]; and (d) the control loops were deactivated when $F_X^{(r)}(k) \cong F_{X,SS}^{(r)}$.

For the direct transition SS2b → SS6b, all the feeds were changed at $t_1 = 0$ (Figure 8a). The set point changes for $\bar{M}_n^{(r)}$ ($r = 1, 2, 3, 4, 7$) were sequentially introduced, as indicated by the step changes in Figs. 8c,d. Figure 8b shows the manipulated CTA feeds. The CTA feeds into reactors 1, 2, 3, and 4 start at their SS2b values and finish at their SS6b values. In contrast, the CTA feed into reactor 7 was only applied during the transient and was otherwise zero. The controllers were adjusted to produce rapid responses and small overshoots or undershoots. Figure 8c and d compares the controlled $\bar{M}_n^{(r)}$ variables with their corresponding set points. In all cases, small undershoots are observed in $\bar{M}_n^{(r)}$, because of the relatively large values of $F_X^{(r)}$ at the beginning of their control actions. Figure 8e−h shows the smoother (and longer) transitions of $\bar{M}_w^{(r)}$ and $x^{(7)}$, and the moderate overshoots and undershoots of the final polydispersity and $\bar{B}_{n3}^{(7)}$. The off-specs are accumulated between $t_2 = 152$ min (when $\bar{M}_n^{(7)}$ becomes 10% lower than its initial SS value) and $t_3 = 594$ min (when $\{\bar{M}_w^{(7)}\}/\{\bar{M}_n^{(7)}\}$ is the last variable to enter into the ±10% specification bands of the final grade).

For the inverse transition SS6b → SS2b, all the reagents suffer a step change at $t_1 = 0$ (Figure 9a). Figure 9c and d compare the controlled $\bar{M}_w^{(r)}$ variables with their corresponding set

Table 3. Changes of Grade between Optimal Steady States: Total Off-Spec Mass and CTA Consumption during the Transient

	SS2b → SS6b		SS6b → SS2b	
transition	off-spec rubber (kg)	CTA consumption (kg)	off-spec rubber (kg)	CTA consumption (kg)
proposed strategy	25800	36.8	18900	14.0
"bang-bang" plant policy[a]	29300	15.1	30700	9.0

[a] Modified by admitting intermediate feeds of comonomers and CTA. Also, the off-specs are calculated with the criterion that all the molecular variables must fall inside ±10% around their desired SS values.

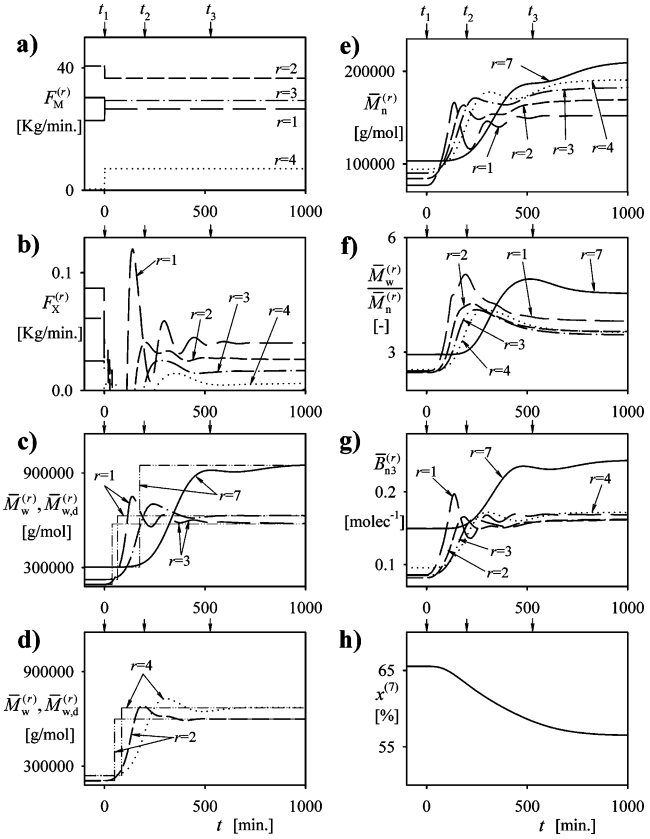

Figure 9. Change of grade from SS6b (grade 1502) to SS2b (grade 1712), with $\bar{M}_w^{(r)}$ control into reactors 1, 2, 3, 4, and 7. The off-spec product is accumulated between $t_2 = 198$ and $t_3 = 510$ min: (a) step change at $t = 0$ of monomer feed into reactors 1, 2, 3, 4, and 7; (b) CTA feed profiles into reactors 1, 2, 3, 4, and 7; (c and d) sequential step changes in the set points of $M_{w,d}^{(r)}$ and the evolution of $\bar{M}_w^{(r)}$ in reactors 1, 2, 3, 4, and 7; (e−g) evolution of $\bar{M}_w^{(r)}$, $\bar{M}_w^{(r)}/\bar{M}_n^{(r)}$ and $\bar{B}_{n3}^{(r)}$ in reactors 1, 2, 3, 4, and 7; and (h) evolution of the final monomer conversion. At $t_1 = 0$ min, a step change in the recipe is introduced.

points. The required CTA feeds are given in Figure 9b. As previously mentioned, the CTA feed profiles into reactors 1, 2, 3, and 4 exhibit transients between their initial and final SSs. However, no CTA feed into reactor 7 is required in this case. The evolutions of the quality variables are qualitatively similar to those of Figure 8. In the first reactors, the molecular weights rapidly respond to their CTA feeds, producing some oscillations in the average molecular properties. In the last reactors, such oscillations are smeared off, and, for example, the final conversion exhibits a slow transition into the final product (see Figure 9h). The off-spec product is accumulated between $t_2 = 198$ min (when $\bar{M}_w^{(7)}$ is the first variable to emerge from the specifications of SS6b); and $t_3 = 510$ min (when $\bar{M}_n^{(7)}$ is the last variable to enter into specifications of SS2b). Note that the molecular-weight oscillations in the first reactor are completely smeared off in the final product. The oscillations in the first reactor could have been attenuated by reducing the controller gains; however, this was discarded because it increased the amount of off-specs.

Table 4. Off- Spec Mass and CTA Consumption in the Investigated Transitions from SS2a to SS6b and Vice Versa (see Figure 5)

transition paths	off-spec rubber (kg)	CTA consumption (kg)
SS2a → SS2b → SS6b	25800	36.8
SS2a → SS6b	32100	53.5
SS6b → SS2b → SS2a	18900	14.0
SS6b → SS2a	20600	18.9

The presented simulations were also compared with adapted versions of the (open-loop and bang-bang) plant policies that include the intermediate feeds. The time evolutions are not presented here, for reasons of space, but Table 3 shows the final off-spec masses and CTA consumptions. The off-specs were estimated with the criterion that all the quality variables should remain inside the ±10% bands around their desired SS values. This criterion provides a mass of intermediate off-specs that is practically coincident with that of industry. Compared with the adapted plant policies for changes of grade, the strategies of Figures 8 and 9 reduce the off-specs by 12% for SS2b → SS6b; and by 38.5% for SS6b → SS2b. However, the proposed closed-loop strategies require increased CTA consumption (see Table 3).

Simultaneous Changes of Production and Grade. Consider the transitions SS2a → SS6b and vice versa. As illustrated in Figure 5, the operations can be performed either in a single step (diagonal paths), or in two steps. In the two-step case, the possible alternatives are as follows: SS2a → SS2b → SS6b, or SS2a → SS6a → SS6b. The single-step transitions can be calculated by simultaneous application of the proposed algorithms (i.e., a closed-loop control for the global calorimetric conversion, and a set of sequential controllers for either $\bar{M}_n^{(r)}$ or $\bar{M}_w^{(r)}$ in reactors 1, 2, 3, 4, and 7). These calculations are straightforward, because of the dynamic decoupling between conversion and the molecular properties. However, sequential transitions are preferable to simultaneous transitions. To see this, remember that the changes in production at a given grade can be implemented with negligible generation of off-specs; and that the off-specs generated during changes of grade requiring a constant production are proportional to the level of production. This suggests that the best strategy is SS2a → SS2b → SS6b and backward; i.e., with the changes of grade performed at the lower level of production. Table 4 compares the off-spec mass and CTA consumption for the four investigated transitions. The sequential strategies are simpler to calculate and apply, and also exhibit lower off-spec masses and CTA consumptions.

Conclusions

In the investigated industrial process, all the reagents are fed into the first reactor. However, there are clear advantages when admitting intermediate feeds of the comonomers mixture and the chain transfer agent (CTA). A two-step calculation procedure was developed to increase the steady-state (SS) production. First,

the total feed rate and the feed flow of comonomer mixture into the first reactors were simultaneously adjusted for reproducing the required final values of conversion and particle diameter. The molecular properties then were adjusted by intermediate addition of CTA. Three control strategies were tested, which involved reproducing the normal SS profiles of either $\bar{M}_n$, $\bar{M}_w$, or $\bar{B}_{n3}$. The SS control of $\bar{M}_w^{(r)}$ proved preferable for reproducing a final molecular characteristics of the normal SS. The SS control of $\bar{B}_{n3}^{(r)}$ reduces the final average molecular weights and degree of branching, which makes it possible to increase the number of continuously stirred tank reactors (CSTRs) in the train (and, therefore, conversion) without deteriorating the rubber quality.

To calculate the SS optimizations, we have taken advantage of the fact that conversion and particle size are practically unaffected by the molecular weights. This allows us to first (i) calculate the comonomer feeds required to increase production, while maintaining fixed values of conversion and particle density, and then (ii) calculate the CTA feeds required to control the molecular characteristics. Alternatively, a more general (but also more complex) calculation procedure is also feasible, involving a simultaneous adjustment of the intermediate feeds of comonomers and CTA, to produce the required values of conversion, particle density, and molecular characteristics.

For changes in production at a fixed rubber grade, the off-specs can be almost eliminated through a regulatory closed-loop control of the global conversion, with manipulation of the total feed flow. In the presented simulations, on-line estimations of the calorimetric conversion were assumed. Calorimetric conversion calculations are feasible in practice, because they can be produced from on-line measurements of the temperatures and evaporated refrigerant flows.

For changes of grade at a given production, the required CTA feeds into reactors 1, 2, 3, 4, and 7 were calculated through a set of virtual controllers, whereas all the other reagents were changed in a step fashion at $t = 0$. The controlled variables were either $\bar{M}_n$ or $\bar{M}_w$, according to whether the molecular weights had to be reduced or increased. The proposed algorithm was simply a mathematical tool for calculating the necessary CTA feed profiles, with the idea of then applying such profiles in an open-loop fashion. The quality of open-loop strategies are totally dependent on the accuracy of the simulation model. In our case, a representative mathematical model was used that was previously verified with SS and dynamic measurements.[17] The readapted (open-loop and "bang-bang") plant policies for changes of production and grade are extremely simple to apply, and also provide quite reasonable results. For changes of production and grade, the best strategy is a sequential transition, with the change of grade being performed at the lower level of production.

Acknowledgment

We thank CONICET, SECyT, and Universidad Nacional del Litoral for the financial support. We are also grateful to Petrobras Energía S.A. for providing us with the industrial data.

Appendix A. Required Chain Transfer Agent Additions for Producing Prespecified Steady-State Profiles of $\bar{M}_n^{(r)}$, $\bar{M}_w^{(r)}$, and $\bar{B}_{n3}^{(r)}$

Molecular Properties Model. For any generic reactor r, the Molecular Weights Module of Gugliotta et al.[17] is reproduced in eqs A.1−A.8:

$$\frac{dN_X^{(r)}}{dt} = \frac{F_X^{(r)}}{M_X} + q_X^{(r-1)}[X]_p^{(r-1)} - q_X^{(r)}[X]_p^{(r)} - k_{fX}[X]_p^{(r)}\, Y_0^{(r)}\, V_p^{(r)} \quad \text{(A.1)}$$

$$\frac{d(V_p^{(r)}\, Q_0^{(r)})}{dt} = [k_{fM}[M]_p^{(r)} + k_{fX}[X]_p^{(r)} + k_{fIm_1}[Im_1]_p^{(r)} - k_p^* Q_1^{(r)}]Y_0^{(r)}\, V_p^{(r)} + q_p^{(r-1)}\, Q_0^{(r-1)} - q_p^{(r)}\, Q_0^{(r)} \quad \text{(A.2)}$$

$$\frac{d(V_p^{(r)}\, Q_1^{(r)})}{dt} = k_p[M]_p^{(r)}\, Y_0^{(r)}\, V_p^{(r)} + q_p^{(r-1)}\, Q_1^{(r-1)} - q_p^{(r)}\, Q_1^{(r)} \quad \text{(A.3)}$$

$$\frac{d(V_p^{(r)}\, Q_2^{(r)})}{dt} = \frac{k_p[M]_p^{(r)} + k_{fX}[X]_p^{(r)} + (k_{fP} + k_p^*)Q_2^{(r)}}{k_{fM}[M]_p^{(r)} + k_{fX}[X]_p^{(r)} + k_{fP}Q_1^{(r)}}\, Y_0^{(r)}\, V_p^{(r)} 2(k_p[M]_p^{(r)} + k_p^*\, Q_2^{(r)}) + q_p^{(r-1)}\, Q_2^{(r-1)} - q_p^{(r)}\, Q_2^{(r)} \quad \text{(A.4)}$$

$$\frac{d(V_p^{(r)}\, Q_0^{(r)}\, \bar{B}_{n3}^{(r)})}{dt} = k_{fP}Q_1^{(r)}\, Y_0^{(r)}\, V_p^{(r)} + q_p^{(r-1)}\, Q_0^{(r-1)}\, \bar{B}_{n3}^{(r-1)} - q_p^{(r)}\, Q_0^{(r)}\, \bar{B}_{n3}^{(r)} \quad \text{(A.5)}$$

with

$$q_X^{(r)} = K_{Xmw}K_{Xwp}q_m^{(r)} + K_{Xwp}q_w^{(r)} + q_p^{(r)} \quad \text{(A.6)}$$

$$[i]_p^{(r)} = \frac{N_i^{(r)}}{K_{imw}K_{iwp}V_m^{(r)} + K_{iwp}V_w^{(r)} + V_p^{(r)}} \quad (\text{for } i = B, S, X, Im_1) \quad \text{(A.7)}$$

$$Y_0^{(r)} = \frac{\bar{n}^{(r)}N_p^{(r)}}{V_p^{(r)}N_{Av}} \quad \text{(A.8)}$$

where $F_X^{(r)}$ is the inlet mass flow of CTA into reactor r; $q_j^{(r)}$ is the total outlet volume flow rate of phase j into reactor r; $q_X^{(r)}$ is the outlet volume flow rate of CTA in reactor r; $N_X^{(r)}$ is the total number of moles of CTA; $[i]_p^{(r)}$ is the molar concentration of i (i = X, M, Im_1) in the polymer phase of reactor r; $\bar{n}^{(r)}$ is the average number of free radicals per particle in reactor r; $N_p^{(r)}$ is the total number of polymer particles in the reactor r; $Y_0^{(r)}$ is the concentration of free radicals in the polymer phase in reactor r; $V_j^{(r)}$ are the volumes of phase j in reactor r; $Q_n^{(r)}$ (n = 0, 1, 2) is the nth moment of the number chain length distribution in reactor r; $\bar{B}_{n3}^{(r)}$ is the number-average number of trifunctional branches per molecule in reactor r; k_p, k_{fM}, k_{fX}, k_{fP}, k_{fIm_1}, and k_p^* are the pseudo-rate constants associated to propagation, chain transfer to the monomer, chain transfer to the CTA, chain transfer to the polymer, chain transfer to the organic deactivating impurity, and propagation with the internal double bonds, respectively; K_{imw}, K_{iwp} are the partition coefficients of i between phases; and N_{Av} is the Avogadro's constant.

The number- and weight-average molecular weights in reactor r ($\bar{M}_n^{(r)}$,$\bar{M}_w^{(r)}$) are calculated from

$$\bar{M}_n^{(r)} = M_{eff}\frac{Q_1^{(r)}}{Q_0^{(r)}} \quad \text{(A.9a)}$$

$$\bar{M}_w^{(r)} = M_{eff}\frac{Q_2^{(r)}}{Q_1^{(r)}}. \quad \text{(A.9b)}$$

where M_{eff} is the effective molar mass of a (hypothetical) average monomer.

Required CTA Feeds. In the SS, the derivatives of eqs A.1−A.5 are zero. To calculate the required feeds of CTA for the SS optimizations involving the control of either $\bar{M}_{\text{n}}^{(r)}$, $\bar{M}_{\text{w}}^{(r)}$, or $\bar{B}_{n3}^{(r)}$, we determined the desired CTA concentration in the polymer phase and in reactor r $[X]_{\text{p,d}}^{(r)}$, for the three possible controls. First, consider reproducing the prespecified SS profile of $\bar{M}_{\text{n}}^{(r)}$, defined by $\bar{M}_{\text{n,d}}^{(r)}$. After introducing eqs A.2 and A.3 into eq A.9a, one obtains

$$[X]_{\text{p,d}}^{(r)} = \left[\frac{M_{\text{eff}}}{\bar{M}_{\text{n,d}}^{(r)}} - \frac{k_{\text{fM}}}{k_{\text{p}}} + \frac{k_{\text{p}}^*}{q_{\text{p}}^{(r)}} Y_0^{(r)} V_{\text{p}}^{(r)}\right]\frac{k_{\text{p}}}{k_{\text{fX}}}[M]_{\text{p}}^{(r)} + \frac{k_{\text{p}}^*}{k_{\text{fX}}} \frac{q_{\text{p}}^{(r-1)} Q_1^{(r-1)}}{q_{\text{p}}^{(r)}} - \frac{k_{\text{fm1}}}{k_{\text{fX}}}[\text{I}_{m1}]_{\text{p}}^{(r)} + \left[\frac{M_{\text{eff}}}{\bar{M}_{\text{n,d}}^{(r)}} - 1\right]\frac{q_{\text{p}}^{(r-1)} Q_0^{(r-1)}}{k_{\text{fX}} Y_0^{(r)} V_{\text{p}}^{(r)}} \quad \text{(A.10)}$$

Now, consider reproducing the prespecified SS profile of $\bar{M}_{\text{w}}^{(r)}$ given by $\bar{M}_{\text{w,d}}^{(r)}$. The required $[X]_{\text{p,d}}^{(r)}$ profile is obtained from eqs A.4, A.3, and A.9b, yielding

$$[X]_{\text{p,d}}^{(r)} = \left\{\left[q_{\text{p}}^{(r-1)} Q_2^{(r-1)} - q_{\text{p}}^{(r)} Q_1^{(r)}\frac{\bar{M}_{\text{w,d}}^{(r)}}{M_{\text{eff}}}\right][k_{\text{fM}}[M]_{\text{p}}^{(r)} + k_{\text{fIm}_1}[I_{\text{m}_1}]_{\text{p}}^{(r)} + k_{\text{fp}}Q_1^{(r)}] + \left[k_{\text{p}}[M]_{\text{p}}^{(r)} + k_{\text{fIm}_1}[I_{\text{m}_1}]_{\text{p}}^{(r)} + (k_{\text{p}}^* + k_{\text{fp}})Q_1^{(r)}\frac{\bar{M}_{\text{w,d}}^{(r)}}{M_{\text{eff}}}\right] Y_0^{(r)} V_{\text{p}}^{(r)} 2\left[k_{\text{p}}[M]_{\text{p}}^{(r)} + k_{\text{p}}^* Q_1^{(r)}\frac{\bar{M}_{\text{w,d}}^{(r)}}{M_{\text{eff}}}\right]\right\} \left\{k_{\text{fX}}\left[q_{\text{p}}^{(r)} Q_1^{(r)}\frac{\bar{M}_{\text{w,d}}^{(r)}}{M_{\text{eff}}} - q_{\text{p}}^{(r-1)} Q_2^{(r-1)} - 2Y_0^{(r)} V_{\text{p}}^{(r)}\left(k_{\text{p}}[M]_{\text{p}}^{(r)} + k_{\text{p}}^* Q_1^{(r)}\frac{\bar{M}_{\text{w,d}}^{(r)}}{M_{\text{eff}}}\right)\right]\right\}^{-1} \quad \text{(A.11)}$$

Finally, consider reproducing the prespecified SS profile of $\bar{B}_{n3}^{(r)}$ given by $\bar{B}_{n3,d}^{(r)}$. The required $[X]_{\text{p,d}}^{(r)}$ is obtained from eqs A.2, A.3, and A.5, yielding

$$[X]_{\text{p,d}}^{(r)} = \frac{1}{k_{\text{fX}}}\left\{[M]_{\text{p}}^{(r)}\left[\frac{k_{\text{p}} Y_0^{(r)} V_{\text{p}}^{(r)} + q_{\text{p}}^{(r-1)} Q_1^{(r-1)}}{q_{\text{p}}^{(r)}}\left(k_{\text{p}}^* + \frac{k_{\text{fp}}}{\bar{B}_{n3,\text{d}}^{(r)}}\right) - k_{\text{fM}}\right] + \frac{q_{\text{p}}^{(r-1)} Q_0^{(r-1)}}{Y_0^{(r)} V_{\text{p}}^{(r)}}\left[\frac{\bar{B}_{n3}^{(r-1)}}{\bar{B}_{n3,\text{d}}^{(r)}} - 1\right]\right\} \quad \text{(A.12)}$$

From $[X]_{\text{p,d}}^{(r)}$ calculated through eqs A.10, A.11, or A.12, the required SS feeds of CTA into reactor r are finally given by

$$F_{\text{X,SS}}^{(r)} = \{[q_{\text{X}}^{(r)} + k_{\text{fX}} Y_0^{(r)} V_{\text{p}}^{(r)}][X]_{\text{p,d}}^{(r)} - q_{\text{X}}^{(r-1)}[X]_{\text{p}}^{(r-1)}\} M_{\text{X}} \quad \text{(A.13)}$$

Appendix B. Reduction of Off-Specs

Changes in Production by Manipulation of the Total Feed Flow. At any discrete time k, the reaction heat rate in reactor r, $Q_R^{(r)}(k)$, is calculated through the following discrete energy balance:[26]

$$Q_R^{(r)}(k) = (C_{p,\text{if}}^{(r)} + \sum_i m_i^{(r)} c_p^i)\frac{T_R^{(r)}(k) - T_R^{(r)}(k-1)}{\Delta t} + q_{\text{T}}^{(r-1)} \rho_l^{(r-1)} c_p^l (T_R^{(r)}(k) - T_{\text{in}}^{(r)}(k)) + \alpha(T_R^{(r)}(k) - T_{\text{a}}(k)) + \lambda F_{\text{ref}}^{(r)}(k) - \beta W_{\text{s}}^{(r)}(k) + \sum_i F_i^{(r)} M_i c_p^i (T_R^{(r)}(k) - T_i^{(r)}(k)) \quad \text{(B.1a)}$$

where $C_{p,\text{if}}^{(r)}$ is the heat capacity of the internal fittings; $m_i^{(r)}$ is the mass of species i (i = B, S, water, copolymer); c_p^i is the specific heat of species i; $T_R^{(r)}$ is the reaction temperature; $\rho_l^{(r)}$ is the latex density; c_p^l is the specific heat of latex; $T_{\text{in}}^{(r)}$ is the inlet flow temperature; λ is the "effective" latent heat of evaporation of the refrigerant mixture; $F_{\text{ref}}^{(r)}$ is the mass flow of refrigerant; $F_i^{(r)}$ is the intermediate mass flow of species i; $T_i^{(r)}$ is the temperature of the intermediate feed flow of species i; α is the global heat transfer coefficient for the heat loss into the environment; β is the stirring heat coefficient; T_{a} is the ambient temperature; and $W_{\text{s}}^{(r)}$ is the stirring power. In our simulated examples, the calorimetric "measurements" $Q_R^{(r)}(k)$ along the train were estimated from

$$Q_R^{(r)}(k) = [R_{\text{pS}}^{(r)}(k)(-\Delta H_{\text{S}}) + R_{\text{pB}}^{(r)}(k)(-\Delta H_{\text{B}})] + \epsilon(k) \quad \text{(B.1b)}$$

with

$$R_{\text{pS}}^{(r)}(k) = \frac{k_{\text{pSS}} k_{\text{pBB}} (r_{\text{S}}[S]_{\text{p}}^{(r)2}(k) + [S]_{\text{p}}^{(r)}(k)[B]_{\text{p}}^{(r)}(k)) Y_0^{(r)}(k) V_{\text{p}}^{(r)}(k)}{k_{\text{pBB}} r_{\text{S}}[S]_{\text{p}}^{(r)}(k) + k_{\text{pSS}} r_{\text{B}}[B]_{\text{p}}^{(r)}(k)} \quad \text{(B.1c)}$$

$$R_{\text{pB}}^{(r)}(k) = \frac{k_{\text{pSS}} k_{\text{pBB}} (r_{\text{B}}[B]_{\text{p}}^{(r)2}(k) + [S]_{\text{p}}^{(r)}(k)[B]_{\text{p}}^{(r)}(k)) Y_0^{(r)}(k) V_{\text{p}}^{(r)}(k)}{k_{\text{pBB}} r_{\text{S}}[S]_{\text{p}}^{(r)}(k) + k_{\text{pSS}} r_{\text{B}}[B]_{\text{p}}^{(r)}(k)} \quad \text{(B.1d)}$$

where ΔH_{S} and ΔH_{B} are the molar polymerization enthalpies of S and B, respectively; R_{pS} and R_{pB} are the consumption rates of S and B, respectively; ϵ is the measurement noise; k_{pSS} and k_{pBB} are the homopropagation rate constants for S and B, respectively; r_{S} and r_{B} are the reactivity ratios of S and B, respectively; and $[S]_{\text{p}}$ and $[B]_{\text{p}}$ are the monomer concentrations in the polymer particles.

The total rate of heat generation is given by the sum of the individual heats:

$$Q_R^{\text{T}}(k) = \sum_{r=1}^{7} Q_R^{(r)}(k) \quad \text{(B.1.e)}$$

The calorimetric conversion x_{c} is calculated from the total heat of reaction, as follows:

$$x_{\text{c}}(k) = \frac{Q_R^{\text{T}}(k)}{\sum_{r=1}^{\text{N}}\left[F_{\text{S}}^{(r)}(k)\frac{(-\Delta H_{\text{S}})}{M_{\text{S}}} + F_{\text{B}}^{(r)}(k)\frac{(-\Delta H_{\text{B}})}{M_{\text{B}}}\right]} \quad \text{(B.2)}$$

The calorimetric conversion x_{c} is regulated by manipulation of the total volume flow rate q_{T}, by application of the following P+I algorithm:

$$q_T(k) = q_{T,SS} + K_{P,1}\left[(\bar{x}_c(k) - x_{c,d}) + \frac{1}{\tau_{I,1}}\sum_{j=1}^{k}(\bar{x}_c(j) - x_{c,d})\Delta t\right] \quad \text{(B.3)}$$

where $K_{P,1}$ and $\tau_{I,1}$ are the controller parameters; $\bar{x}_c(j)$ is a time-averaged calorimetric conversion in the time interval $[j, j+1]$; $x_{c,d}$ is the desired value of x_c; and $q_{T,SS}$ is the total volumetric feed flow of the initial SS (i.e., before the transition).

Changes of Grade by Manipulation of the CTA Feeds. In reactor r, the average molecular weights $\bar{M}_n^{(r)}$ and $\bar{M}_w^{(r)}$ are determined through eqs A.2, A.3, A.4, A.8, and A.10. The necessary CTA feeds $F_X^{(r)}$ for controlling $\bar{M}_n^{(r)}$ or $\bar{M}_w^{(r)}$ were calculated through the following "virtual" P+I controllers:

(a) To reduce the average molecular weights:

$$F_X^{(r)}(k) = F_{X,SS}^{(r)} + K_{P,2}^{(r)}\left\{[\bar{M}_n^{(r)}(k) - \bar{M}_{n,d}^{(r)}] + \frac{1}{\tau_{I,2}^{(r)}}\sum_{z=1}^{k}[\bar{M}_n^{(r)}(z) - \bar{M}_{n,d}^{(r)}]\Delta t\right\} \quad \text{(B.4)}$$

(b) To increase the average molecular weights:

$$F_X^{(r)}(k) = F_{X,SS}^{(r)} + K_{P,2}^{(r)}\left\{[\bar{M}_w^{(r)}(k) - \bar{M}_{w,d}^{(r)}] + \frac{1}{\tau_{I,2}^{(r)}}\sum_{z=1}^{k}[\bar{M}_w^{(r)}(z) - \bar{M}_{w,d}^{(r)}]\Delta t\right\} \quad \text{(B.5)}$$

where $F_{X,SS}^{(r)}$ is the initial CTA flow estimated with eq A.13.

Nomenclature

$\bar{B}_{n3}^{(r)}$ = number-average number of trifunctional branches per molecule

c_p^i = specific heat of reagent i (i = B, S, X, copolymer, and water) (kJ/(kg °C))

c_p^l = specific heat of the latex (kJ/(kg °C))

$C_{p,if}^{(r)}$ = heat capacity of the internal fittings of reactor r (kJ/°C)

C_p^i = heat capacity of reagent i (i = B, S, X, copolymer, and water) (kJ/°C)

$\bar{d}_p^{(r)}$ = unswollen number-average particle diameter (nm)

$F_i^{(r)}$ = mass flow of reagent i (i = B, S, X) (kg/min)

$F_M^{(r)}$ = additional mass flow of the comonomers mixture into reactor r (kg/min)

$F_{ref}^{(r)}$ = mass flow of refrigerant (kg/min)

G = polymer production (kg/min)

$[i]_p^{(r)}$ = molar concentration of species i (i = B, S, X, I_{m1}) in the polymer phase (mol/L)

I_{m_1} = deactivating organic impurity

$k = (t/\Delta t)$ = discrete time

$k_{fl_{m1}}$ = pseudo-rate constant of chain transfer to I_{m1}

k_{fM} = pseudo-rate constant of transfer to the monomer (L/(mol min))

k_{fp} = pseudo-rate constant of transfer to the polymer (L/(mol min))

k_{fX} = pseudo-rate constant of transfer to the CTA (L/(mol min))

K_{imp} = partition coefficient of reagent i (i = S, B, X) between the monomer phase and the polymer phase

K_{iwp} = partition coefficient of reagent i (i = S, B) between the aqueous phase and the polymer phase

$K_{P,1}$ = proportional gain of the P+I controller in eq B.3 (L/min)

$K_{P,2}^{(r)}$ = proportional gain of the P+I controllers in reactor r in eqs B.4 and B.5 (mol/min)

k_p = pseudo-rate constant of propagation in the polymer phase (L/(mol min))

k_p^* = pseudo-rate constant of reaction with internal double bonds (L/(mol min))

k_{pSS}, k_{pBB} = homopropagation rate constants in the polymer phase (L/(mol min))

M = monomers B and S

M_B = molecular weight of B; M_B = 54.09 (g/mol)

M_{eff} = effective molecular weight of an average repeating unit (g/mol)

M_S = molecular weight of S; M_S = 104.15 (g/mol)

$m_i^{(r)}$ = mass of reagent i (i = B, S, copolymer, water, and initiator) in reactor r (kg)

$\bar{M}_n^{(r)}$, $\bar{M}_w^{(r)}$ = number- and weight-average molar masses in reactor r (g/mol)

$[M]_p^{(r)}$ = total monomer concentration in the polymer phase ($[B]_p^{(r)} + [S]_p^{(r)}$) in reactor r (mol/L)

M_X = molecular weight of the CTA (*tert*-dodecylmercaptan); = 202.4 g/mol

N_{Av} = Avogadro's constant (mol^{-1})

$N_i^{(r)}$ = moles of reagent i (i = B, S, X) in reactor r (mol)

$N_p^{(r)}$ = total number of polymer particles in reactor r

$\bar{n}^{(r)}$ = average number of free radicals per latex particle in reactor r

$\bar{p}_S$ = average mass fraction of polymerized S in the copolymer

$q_i^{(r)}$ = outlet volume flow rate of reagent i (i = B, S, X) (L/min)

$q_j^{(r)}$ = outlet volume flow rate of phase j (j = m, p, w) (L/min)

q_T = total volume flow in the train (L/min)

$Q_n^{(r)}$ = nth (n = 0, 1, 2) moment of the number chain-length distribution in reactor r (mol/ L)

$Q_R^{(r)}$ = reaction heat rate in reactor r (kJ/min)

Q_R^T = total reaction heat (kJ/min)

r_B, r_S = reactivity ratios of B and S

$R_{pB}^{(r)}$, $R_{pS}^{(r)}$ = consumption rates of B and S in reactor r (mol/min)

t = time (min)

T_a = ambient temperature (°C)

$T_i^{(r)}$ = temperature of inlet flow of reagent i into reactor r (i = B, S, X) (°C)

$T_{in}^{(r)}$ = inlet flow temperature into reactor r (°C)

$T_R^{(r)}$ = reaction temperature in reactor r (°C)

$V_j^{(r)}$ = phase volume j (j = m, p, w) in reactor r (L)

$W_s^{(r)}$ = stirring power in reactor r (kJ/min)

x_c = calorimetric conversion

x = gravimetric conversion

x_{sol} = solid contents

X = chain transfer agent, CTA

$[X]_{p,d}^{(r)}$ = desired molar concentration of CTA in polymer phase, for producing a prespecified average molecular property in reactor r (mol/L)

$Y_0^{(r)}$ = concentration of free radicals in the polymer phase of reactor r (mol)

Greek Symbols

α = global heat-transfer coefficient for the heat loss into the environment (J/(K min))
β = stirring heat coefficient
ϵ = additive measurement noise (kJ/min)
$\rho_l^{(r)}$ = latex density in reactor r (kg/m^3)
φ_S = fraction of S-terminated radicals
λ = "effective" latent heat of vaporization of the refrigerant (a propane−propylene mixture) (J/g)
$\tau_{I,1}$ = integral time of the P+I controller in eq B.3 (min)
$\tau_{I,2}^{(r)}$ = integral time of the P+I controllers in reactor *r* in eqs B.4 and B.5 (min)
Δt = time interval between consecutive measurements (min)
ΔH_B ΔH_S = respective molar polymerization enthalpies of B and S (J/mol)

Superscripts

r = reactor number

Subscripts

d = indicates desired value (or set point)
m = indicates monomer droplets phase
p = indicates particles phase
w = indicates aqueous phase

Literature Cited

(1) Kirk, R. E.; Othmer, D. F. *Encycl. Chem. Technol.* **1981**, *8*, 608.

(2) Blackley, D. C. Diene-based Synthetic Rubbers. In *Emulsion Polymerization and Emulsion Polymers*; Lovell, P. A., El-Aasser, M. S., Eds.; Wiley: New York, 1997.

(3) Poehlein, G. W.; Dougherty, D. J. Continuous Emulsion Polymerization. *Rubber Chem. Technol.* **1977**, *50*, 601.

(4) Kensuke, O.; Tsutomu, H.; Mitsuru, M.; Tooru, T.; Mitsutoshi, F.; Nobuyuki, B. Estimation Method of Mooney Viscosity, Jpn. Patent No. JP52145080, 1977.

(5) Nobuo, T. Estimation of Mooney Viscosity, Jpn. Patent No. JP59048642, 1984.

(6) Saldívar, E.; Dafniotis, P.; Ray, W. H. Mathematical Modeling of Emulsion Copolymerization Reactors. I. Model Formulation and Application to Reactors Operating with Micellar Nucleation. *J. Macromol. Sci.−Rev. Macromol. Chem. Phys.* **1998**, *C38*, 207.

(7) Arzamendi, G.; Sayer, C.; Zoco, N.; Asua, J. M. Modeling of MWD in Emulsion Polymerization: Partial Distinction Approach. *Polym. React. Eng.* **1998**, *6* (3−4), 193.

(8) Gao, J.; Penlidis, A. Mathematical Modeling and Computer Simulator/Database for Emulsion Polymerization. *Prog. Polym. Sci.* **2002**, *27*, 403.

(9) Salazar, A.; Gugliotta, L. M.; Vega, J. R.; Meira, G. R. Molecular Weight Control in a Starved Emulsion Polymerization of Styrene. *Ind. Eng. Chem. Res.* **1998**, *37*, 3582.

(10) Echevarría, A.; Leiza, J.; de la Cal, J.; Asua, J. M., Molecular Weight Distribution Control in Emulsion Polymerization. *AIChE J.* **1998**, *44* (7), 1667.

(11) Vicente, M.; BenAmor, S.; Gugliotta, L. M.; Leiza, J. R.; Asua, J. M. Control of Molecular Weight Distribution in Emulsion Polymerization Using On-Line Reaction Calorimetry. *Ind. Eng. Chem. Res.* **2001**, *40*, 218.

(12) Gugliotta, L. M.; Salazar, A.; Vega, J. R.; Meira, G. R. Emulsion Polymerization of Styrene. Use of *n*-Nonyl Mercaptan for Molecular Weight Control. *Polymer* **2001**, *42* (79), 2719.

(13) Kanetakis, J. Simulation of a Styrene/Butadiene Rubber Production in a Continuous Stirred Tank Reactor Train: Modelling of Particle Size Distributions, M. Eng. Thesis, McMaster University, Hamilton, Ontario, Canada, 1984.

(14) Broadhead, T. Dynamic Modeling of the Emulsion Copolymerization of Styrene/Butadiene, M. Eng. Thesis, McMaster University, Hamilton, Ontario, Canada, 1984.

(15) Broadhead, T. O.; Hamielec, A. E.; MacGregor, J. F. Dynamic Modelling of the Batch, Semibatch and Continuous Production of Styrene/Butadiene Copolymers by Emulsion Copolymerization. *Makromol. Chem.* **1985**, *Suppl*. 10/11, 105−128.

(16) Kozub, D. J. Multivariable Control: Design, Robustness and Nonlinear Inferencial Control of Semibatch Polymerization Reactors. Ph.D. Thesis, McMaster University, Hamilton, Ontario, Canada, 1989.

(17) Gugliotta, L. M.; Brandolini, M. C.; Vega, J. R.; Iturralde, E. O.; Azum, J. M.; Meira, G. R. Dynamic Model of a Continuous Emulsion Copolymerization of Styrene and Butadiene. *Polym. React. Eng.* **1995**, *3* (3), 201.

(18) Ueda, T.; Omi, S.; Kubota, H. Experimental Study of Continuous Emulsion Polymerization of Styrene. *J. Chem. Eng. Jpn.* **1971**, *4* (1), 50.

(19) Nomura, M.; Kojima, H.; Harada, M.; Eguchi, W.; Nagata, S. Continuous Flow Operation in Emulsion Polymerization of Styrene. *J. Appl. Polym. Sci.* **1971**, *15*, 675.

(20) Hamielec, A. E.; MacGregor, J. F. *Modeling Copolymerizations—Control of Composition, Chain Microstructure, Molecular Weight Distribution, Long Chain Branching and Cross-linking*; Polymer Reaction Engineering—Berlin International Workshop; Reichert, K. H., Geiseler, W., Eds.; VCH Publisher: Berlin, 1983.

(21) Penlidis, A.; MacGregor, J. F.; Hamielec, A. E. Dynamic Modeling of Emulsion Polymerization Reactors. *AIChE J.* **1985**, *31*, 881.

(22) Kanetakis, J.; Wong, F. Y.; Hamielec, A. E.; MacGregor, J. F. Steady-State Modeling of a Latex Reactor Train for the Production of Styrene−Butadiene Rubber. *Chem Eng. Commun.* **1985**, *35*, 123.

(23) Vega, J. R.; Gugliotta, L. M.; Brandolini, M. C.; Meira, G. R. Steady-State Optimization in a Continuous Emulsion Copolymerization of Styrene and Butadiene. *Lat. Am. Appl. Res.* **1995**, *25*, 207.

(24) Gugliotta, L. M.; Vega, J. R.; Antonione, C. E.; Meira, G. R. Emulsion Copolymerization of Acrylonitrile and Butadiene in an Industrial Batch Reactor. Estimation of Conversion and Polymer Quality from On-line Energy Measurements. *Polym. React. Eng.* **1999**, *7* (4), 531.

(25) Vega, J. R.; Gugliotta, L. M.; Meira, G. R. Continuous Emulsion Polymerization of Styrene and Butadiene. Reduction of Off-Spec Product between Steady-States. *Lat. Am. Appl. Res.* **1995**, *25*, 77.

(26) Vega, J. R.; Gugliotta, L. M.; Meira, G. R. Emulsion Copolymerization of Acrylonitrile and Butadiene. Semi-Batch Strategies for Controlling Molecular Structure on the Basis of Calorimetric Measurements. *Polym. React. Eng.* **2002**, *10* (1&2), 59.

Received for review April 20, 2005
Revised manuscript received August 19, 2005
Accepted October 13, 2005

IE0504755